



Cite this: *React. Chem. Eng.*, 2025, 10, 2669

Assessing the viability of energetic valorization of textile waste through fluidized bed catalytic combustion with carbon capture

Walter Fernández Benítez, ^a
Einar Blanco Machin ^{*b} and Daniel Travieso Pedroso ^c

The textile industry is one of the most harmful to the environment due to the large amount of waste it generates, which usually ends up in landfills or is incinerated, as happened in 2015, when 73% of the textiles produced worldwide were disposed of in these ways. This study evaluates the feasibility of energetically valorizing textile waste through catalytic combustion with zeolite in fluidized bed and carbon capture, using Aspen Plus® software. The simulation shows that textile waste can be combusted, ultimately reducing NO_x to N₂ and capturing about 40% of CO₂. Furthermore, catalytic combustion has an overall efficiency of 40%, and oxy-combustion has an efficiency of only 18%, attributable to the energy consumption of the N₂ air separation stage. This study is a starting point for the energetic valorization of textile waste in an environmentally responsible manner.

Received 26th May 2025,
Accepted 6th August 2025

DOI: 10.1039/d5re00234f

rsc.li/reaction-engineering

1. Introduction

The textile industry is the second most harmful industry to the environment, after the oil industry, due to the large amounts of water and energy consumed in the manufacturing of textiles and also due to the waste generated during production.¹

Between 2000 and 2020, global textile production nearly doubled, increasing from 58 million tons to 109 million tons. An increase of up to 145 million tons of production is projected for 2030.² In 2015, of the total production worldwide, 73% was disposed of in landfills or incinerated.³

In Europe, nearly 26 kg of textiles are used per person, and about 11 kg are discarded yearly. Most used clothing in Europe (87%) is incinerated or disposed of in landfills, and only 1% of used clothing is recycled into new clothing.² In the United States, the textile recovery rate is around 15% of production.⁴

Textile consumption in Chile has increased in the last 20 years, increased from an average of 13 purchases per person in 2015 to 50 in 2020. In 2018, each inhabitant produced approximately 30 kg of textile waste, reaching 572 118 tons per year of textile waste in the country. In 2021, 156 thousand

tons of used or unused textiles were imported, of which 94 thousand tons ended up in illegal landfills.⁵

The composition of textile waste is highly heterogeneous, typically natural fibers (cotton, hemp, coconut, wool, among others) and synthetic fibers (polyester, nylon, polyurethane, viscose, among others) or a mixture of both.⁶

Current textile waste management strategies include recycling textile fiber to produce new textile products, reusing textile products, biodegrading, disposing of landfills, and valorizing through thermochemical conversion processes.⁷

Combustion is the predominant treatment method for textile waste, and the major challenge of combustion is the high carbon content of flue gas.⁸ In the particular case of textiles, another critical challenge is that flue gases are rich in other chemical compounds or elements, such as CO₂, NO_x, N₂O, SO₂, CO, NH₃, Cl, dioxins, furans, VOC's, dust and heavy metals.⁹ However, this depends on the conditions of the combustion process and emission control.¹⁰

The combustion of textile waste (cotton and polyester) in a fixed-bed reactor was previously studied.¹¹ Among the main results was that the ignition progressed unevenly at low airflow rates and left a significant amount of unburned and partially charred materials. As the air supply increased, the progress of the ignition front became less irregular, increasing the efficiency of the process.

In catalytic combustion, the residues are oxidized to CO₂ and H₂O, and a catalyst is used to decrease the activation energy, which occurs at a lower temperature than in non-catalytic combustion. Catalysts used in combustion systems to control gaseous organic compounds are usually precious or

^a Departamento de Ingeniería de Procesos y Bioproductos, Facultad de Ingeniería, Universidad del Bío – Bío, Av. Collao 1202, Concepción, Chile

^b Departamento de Ingeniería Mecánica (DIM), Facultad de Ingeniería, Universidad de Concepción, Edmundo Larenas 219, Concepción, Chile. E-mail: eblanco@udec.cl

^c Departamento de Ingeniería Mecánica (DIMEC), Facultad de Ingeniería, Universidad del Bío – Bío, Av. Collao 1202, Concepción, Chile



base metals or metal salts. Catalysts can be supported on inert materials, such as alumina (Al_2O_3) or ceramics. For waste destruction, because of their heterogeneity, highly active but non-selective catalysts are required.¹² Catalytic studies show that the simultaneous catalysis of NO_x , dioxins, and furans in flue gas using an experimental system designed with $\text{VO}_x/\text{WO}_x/\text{TiO}_2$ catalysts and alternatives such as zeolites and MnO_x indicates that polymeric VO_x species are effective for NO_x reduction. In contrast, monomeric species favor the oxidation of compounds such as dichlorobenzene, noting that the efficiency depends on the operating temperature.¹³

Carbon capture and storage (CCS) is a key strategy to reduce CO_2 emissions in combustion-based industrial processes.¹⁴ In this context, *in situ* CO_2 capture using adsorbent materials such as calcium oxide (CaO) in fluidized bed reactors has been explored, especially to enrich hydrogen production in syngas. However, the use of CaO presents challenges such as deactivation by thermal and chemical sintering, as well as loss of material by elutriation.¹⁵

In waste treatment by combustion, the predominant combustion is grate combustion. However, fluidized bed combustion has significant advantages: a wide variety of fuel or waste handling, higher combustion efficiency due to better air/waste mixing, lower pollutant emissions due to more efficient combustion, lower ash production due to higher combustion efficiency, higher energy recovery from the waste, higher heat retention of the fluidized bed compared to grate combustion, and higher energy recovery from the waste.¹⁶

Previous studies have explored fixed bed combustion of textiles,^{11,17} pyrolysis or gasification,^{1,18–20} but none have evaluated the synergy between fluidized bed catalytic combustion and CO_2 capture in the same process. This work proposes an innovative approach that combines the use of zeolite as a catalyst for NO_x reduction and CaO as a CO_2 capture agent, which overcomes limitations associated with pollutant emissions in traditional configurations. The combination of these technologies improves energy efficiency, reduces emissions, and helps prepare the industry for increasingly strict environmental regulations.

This study provides a technical assessment of catalytic combustion and oxy-combustion of textile waste with carbon capture. A process simulation is conducted to evaluate its feasibility, and the flue gas composition is compared with reference data to assess environmental impact and efficiency.

2. Methodology

2.1 Scope of the study

This study is based exclusively on process simulations performed in Aspen Plus®. Three textile waste combustion scenarios are considered: one referential (fixed bed, taken from literature) and two developed by simulation (catalytic fluidized bed and catalytic oxy-combustion with carbon capture). The operational parameters are based on previous studies to represent real conditions.

2.2 Technical assessment

Three configurations are compared: (i) fixed-bed combustion, (ii) catalytic fluidized-bed combustion, and (iii) simulation of catalytic oxy-combustion of textile waste in a fluidized-bed reactor with carbon capture. The purpose is to evaluate the impact of catalytic combustion, catalytic oxy-combustion, and carbon capture in reducing pollutant emissions and improving process efficiency.

Case 1: combustion of textile waste in a fixed bed reactor (experimental reference). The baseline for this comparison is the combustion of textile waste in a fixed-bed reactor;¹¹ a fixed-bed reactor is selected because it is the traditional method of waste combustion. The textiles that were combusted in a fixed bed were cotton and polyester. The reactor used for the study was made of 8 mm thick nickel alloy, with a height of 1.5 m and an outer diameter of 20 cm, with an insulation layer of 80 mm and mounted in a 30 mm thick stainless steel casing. Flue gases were collected from the reactor's top and measured in a $\text{CO}_2/\text{CO}/\text{O}_2$ analyzer.

For the study, a mixture of cotton and polyester was considered textile waste. The elemental and proximate analyses are shown in Table 1. Additionally, the elemental analysis and proximate analysis of the 50/50 cotton/polyester blend are shown in Table 1 for reference.

The experimental reference configuration is illustrated in Fig. 1. Textile waste (50/50 cotton/polyester blend, cut into 30×50 mm pieces) is fed to a batch fixed-bed reactor equipped with thermocouples and a gas analyzer. Primary air is injected from the bottom at velocities between $117\text{--}1638 \text{ kg m}^{-2} \text{ h}^{-1}$, while a cyclone separates the residual solids.

Case 2: simulation of catalytic combustion of textile waste in a fluidized bed reactor with carbon capture. Fig. 2 shows a process diagram of the proposed application, fluidized bed catalytic combustion of textile waste with carbon capture. The size reduction process is used as a pretreatment of textile waste, to bring it to sizes reported in the literature of 30×50 mm and density of 90 kg m^{-3} in similar applications.¹¹ They are fed to a fluidized bed reactor, employing zeolite as a catalyst; air is supplied to lift the bed with a forced draft fan and to supply oxygen to the combustion. Energy is harnessed from the flue gases to produce superheated steam; ash is

Table 1 Elemental and proximate analysis of textile wastes

Attribute	Component	Cotton ¹	Polyester ¹	Cotton/polyester ²¹
Element analysis (wt%)	Carbon	48.9	62.5	54.5
	Hydrogen	4.02	4.1	5.6
	Oxygen	45.3	33.3	38.7
	Nitrogen	0.81	0.70	0.4
	Sulfur	0.88	0.82	0.3
Proximate analysis (wt%)	Moisture	0.59	2.17	1.8
	Ash	1.11	2.28	0.7
	Volatile	88.97	88.94	89.2
Higher heating value (MJ kg ⁻¹)	HHV	18.7	22.5	20.5



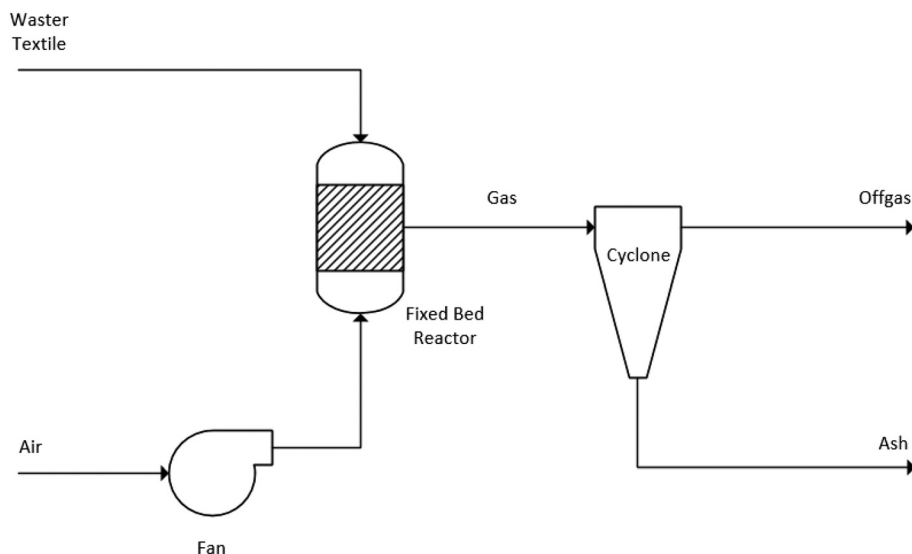


Fig. 1 Fixed bed combustion of textile waste.

removed using a cyclone and a bag filter, and carbon capture is performed in a CaO bed. The flue gases leaving the carbon capture stage are removed from the atmosphere through a stack.

Case 3: simulation of catalytic oxy-combustion of textile waste in a fluidized-bed reactor with carbon capture. Fig. 3 shows a diagram of catalytic oxy-combustion of textile waste with carbon capture, in contrast to Fig. 2, an air separator unit supplies oxygen-enriched air for combustion.

The downstream process continues in the same way as the process in Fig. 2. Supplying oxygen-enriched air subsequently

facilitates the separation and storage of CO₂ from the combustion gases.

In both cases, a general mass balance is reported, and a comparison of the combustion gases (CO₂, CO, and O₂) is made, taking as a reference the case, which corresponds to the combustion of textile waste in a fixed bed reactor.

2.3 Description of simulated process

Fig. 4 shows a PFD diagram of the proposed process for catalytic combustion of textile waste in a fluidized bed with carbon

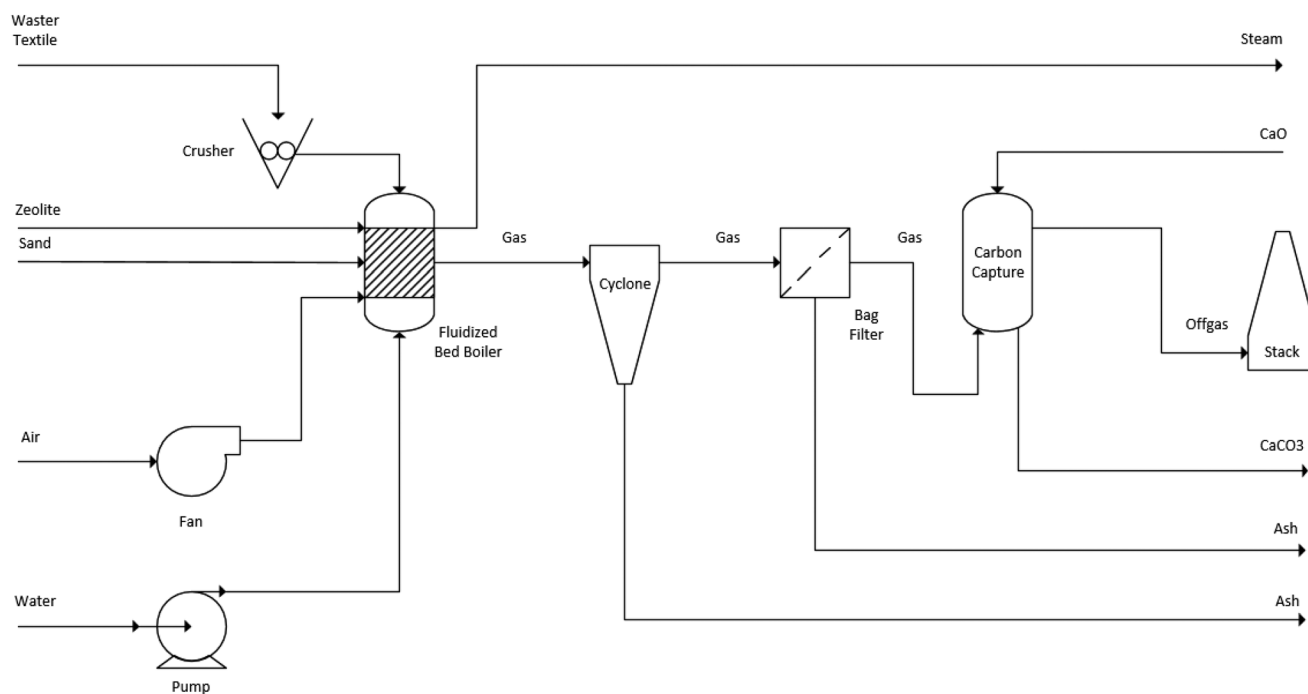


Fig. 2 Fluidized bed catalytic combustion process diagram with carbon capture.



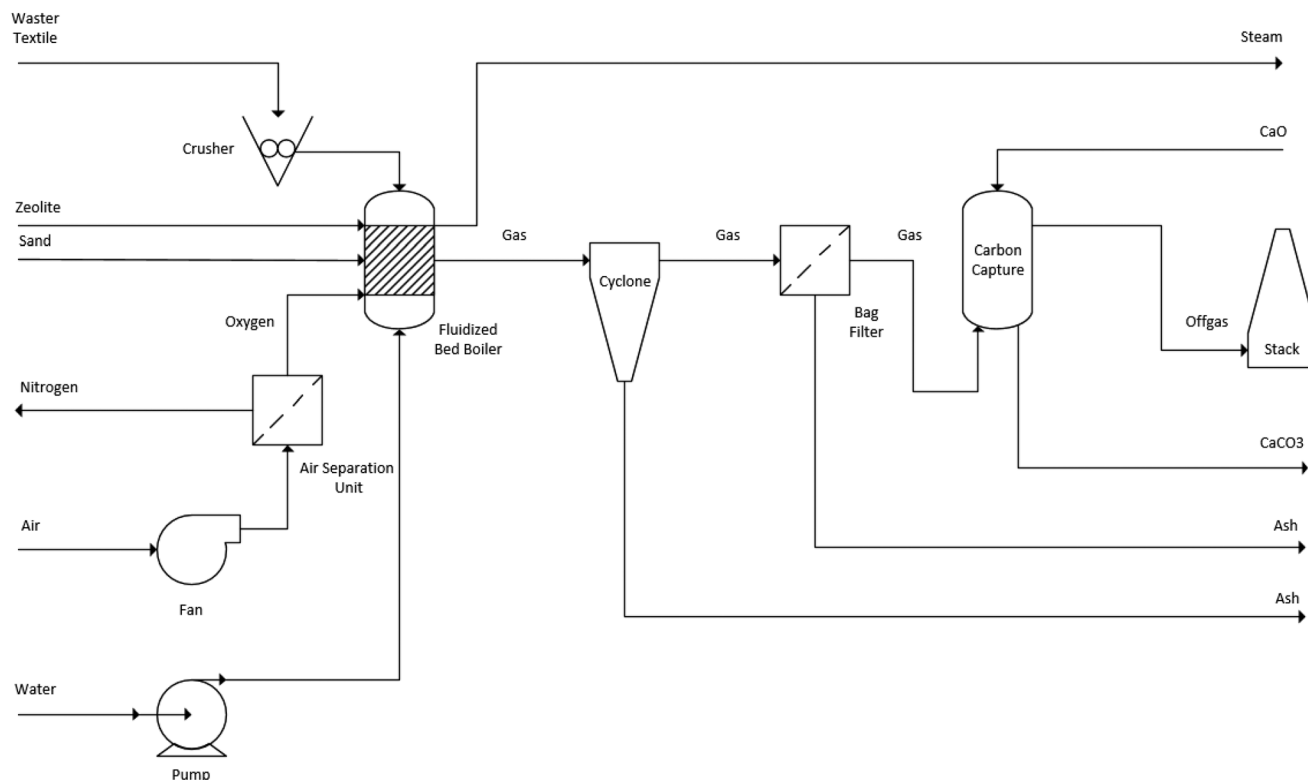


Fig. 3 Fluidized bed catalytic oxy-combustion process diagram with carbon capture.

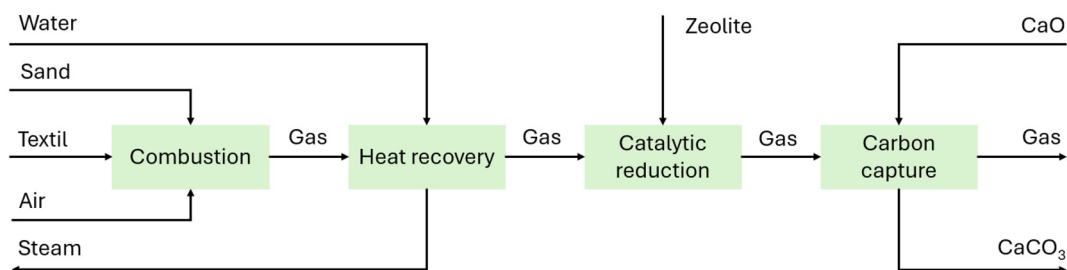


Fig. 4 Process diagram of catalytic fluidized bed combustion of textile waste with carbon capture.

capture. The textile wastes, mainly cotton and polyester, are fed dry to a reactor operating at 1000 °C and 2 bar,²² where the textile combustion reaction occurs. The sand acts as a bed material, increasing the combustion reaction's efficiency,¹⁶ and air in excess of 10% of the stoichiometric air quantity is fed. The flue gases pass through a boiler fed by water at 85 °C; the water is gradually heated to superheated steam. The cold combustion gases enter a reactor operating at 150 °C and 2 bar (ref. 23) to catalytically reduce NO_x (SCR process), using zeolite as a catalyst.¹³ Subsequently, the combustion gases enter a carbon capture process, where CaO is used to capture CO₂.¹⁵ Finally, the gases are eliminated from the atmosphere.

2.4 Model configuration in Aspen Plus

Fig. 5 shows the process flow diagram in Aspen Plus for catalytic combustion of textile waste in a fluidized bed with

carbon capture. The textile waste used as feedstock is converted from unconventional components without a defined chemical formula to conventional components in the ELEMENT1 and ELEMENT2 blocks and then enters the REACTOR, where the combustion reaction, corresponding to an RGibbs block, takes place (it is worth mentioning that in real life, the ELEMENT and RGibbs blocks are a single unit). The minimization of the Gibbs free energy controls the equilibrium of the chemical reactions and the temperature specifications. The flue gases are utilized by a series of heat exchangers (SH1-2, WALL, EC1-2), modeled with HeatX blocks, where water feeds the heat exchangers, and superheated steam is obtained. Using a zeolite catalyst, the SCR process treats the flue gas leaving EC1-2 through an RGibbs block to reduce NO_x to N₂. Ash is removed by an SSplit block called CYCLONE, and finally, carbon capture occurs in a Sep block called CAPTURE, which separates CO₂ using CaO.



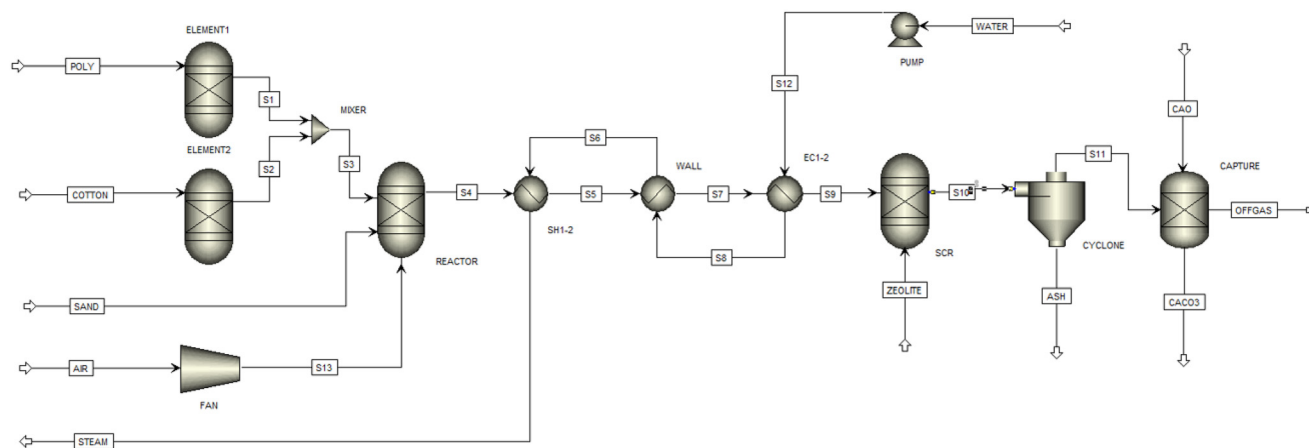


Fig. 5 Aspen Plus process diagram of catalytic combustion of textile waste in a fluidized bed with carbon capture.

Fig. 6 shows the Aspen Plus process flow diagram of catalytic oxy-combustion of textile waste in a fluidized bed with carbon capture; the main difference concerning the process in Fig. 5 is that a Sep block, called SEP, is used to separate the nitrogen from the air so that the combustion is carried out with oxygen-enriched air.

Table 2 presents the names and functions of the blocks within the model.

2.5 Simulation assumptions and parameters

The simulations used the “International System of Units of Measurement” and incorporated the “MIXCINC” process unit category, combining non-conventional and conventional components. Textiles and ash were represented using non-conventional components, while gases and water were represented with conventional components. The performance prediction is based on Gibbs free energy.

Although deviations from equilibrium may exist in complex combustion processes, the models can provide valuable basic predictions, help researchers and engineers

understand the results of reactions under ideal conditions, and provide a reference for further out-of-equilibrium studies.

The density and calorific value of the textiles were determined using the HCOMB and DENGEM models. Simulations were performed using the Peng–Robinson equation of state (PENG-ROB). This method mainly simulates complex thermodynamic systems, especially in biomass conversion, petrochemicals, and natural gas processing. Component yields in the RYield blocks were estimated using FORTRAN. Throughout this process, ash and sand are treated as inert substances without participating in the reaction.

The primary textile feedstock used in the combustion process is residue, which is considered a non-conventional component within the Aspen Plus model. Table 1 explains the higher calorific value, proximate analysis, and elemental analysis of the feedstock obtained from experimental investigations.

The key assumptions of the model are as follows:

Waste size and homogeneity: textile waste was considered to have a small particle size and homogeneous distribution,

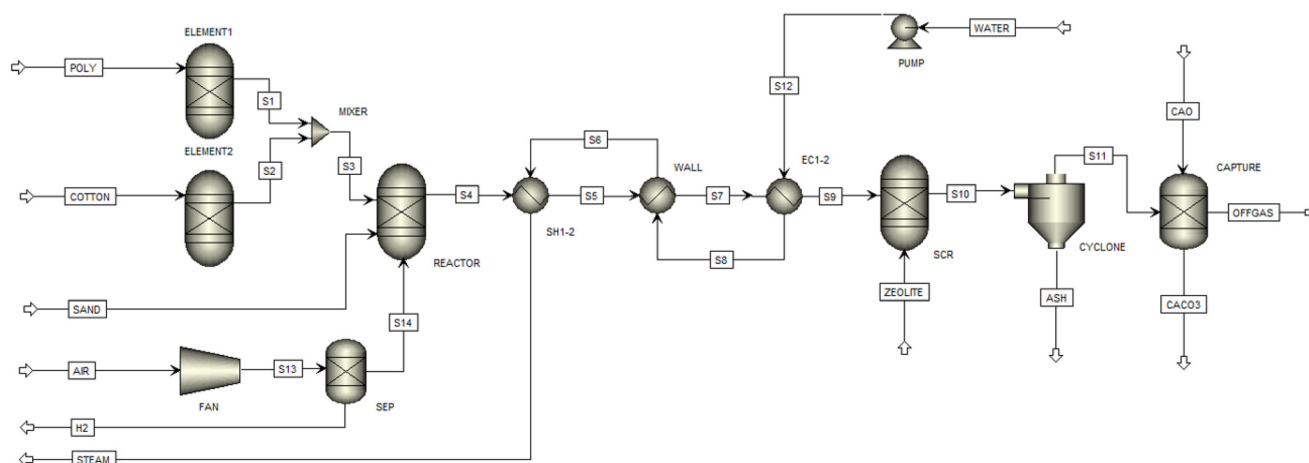


Fig. 6 Aspen Plus process diagram of catalytic oxy-combustion of textile waste in a fluidized bed with carbon capture.



Table 2 Description of the blocks used in process simulation

Block name	Module	Specifications	Description
ELEMENT1	RYield	Temperature: 1000 °C Pressure: 2 bar	Conversion of raw materials from non-conventional components to conventional components
ELEMENT2	RYield	Temperature: 1000 °C Pressure: 2 bar	Conversion of raw materials from non-conventional components to conventional components
MIXER	Mix	N/A	Mix feed to the REACTOR
REACTOR	RGibbs	Temperature: 1000 °C 1200 °C Pressure: 2 bar	Combustion and oxy-combustion reactions are simulated using the Gibbs free energy principle
FAN	Compr	Pressure: 3.5 bar	Feed air to the REACTOR
SH1-2	HeatX	Hot temperature: 600 °C	Heat exchange between water and combustion gases
WALL	HeatX	Hot temperature: 400 °C	Heat exchange between water and combustion gases
EC1-2	HeatX	Hot temperature: 150 °C	Heat exchange between water and combustion gases
PUMP	Pump	Pressure: 11 bar	Feed and increase the water pressure to EC1-2
SCR	RGibbs	Temperature: 150 °C Pressure: 2 bar	Selective catalytic reduction is simulated using the Gibbs free energy principle
CYCLONE	SSplit	N/A	Separate ash from the flue gas stream
CAPTURE	Sep	N/A	Separate a fraction of CO ₂ from flue gases
SEP	Sep	N/A	Enriching air with oxygen for oxy-combustion

ignoring agglomeration effects in the bed and ensuring uniform combustion.¹⁶

Fluidized bed: turbulence is assumed inside the reactor, with good mixing of gases and solids guarantees rapid homogenization of temperature and composition.²⁴

Steady state: the model assumes steady state operation, which allows performance to be evaluated under continuous operating conditions.

Thermodynamic equilibrium: the combustion reactions were modeled under chemical equilibrium (RGibbs module), which implies that the combustion gases reach ideal composition at the given temperatures.

Fixed capture and conversion efficiencies: the CO₂ capture was set at 40%, based on the theoretical capacity of the adsorbent and the percentage of useful lime reported in the literature.²⁵ Catalytic NO_x reduction with zeolite was assumed complete, consistent with experimental data.¹³

Energy losses: heat losses due to radiation or convection in the reactor, piping, and heat exchangers were neglected.

2.6 Process efficiency

For the case of catalytic combustion and oxy-combustion of textile waste in a fluidized bed with carbon capture, the process efficiency (η) is calculated according to eqn (1).

$$\eta = \frac{\sum_i^n E_{\text{out}}}{\sum_i^n E_{\text{in}}} \times 100\% \quad (1)$$

where E represents the energy entering and leaving the system, respectively.

Water and steam energy data were obtained respectively from steam tables,²⁶ energy consumed by equipment such as pumps and fans was obtained from the Aspen Plus software, and the calorific value of the textile wastes was obtained from

ref. 1 and 21. For the energy consumed in the separation of N₂ from air, 0.2 kWh kg⁻¹ O₂ was considered.²⁷

3. Results and discussion

Fig. 7 shows an overall diagram of the combustion process for the material inputs and outputs to calculate the overall material balances of the process.

Table 3 shows an overall mass balance delivered by the simulation model of fluidized bed catalytic combustion of textile waste with carbon capture.

Fig. 8 shows the overall diagram of the oxy-combustion process for the material inputs and outputs to calculate the overall material balances of the process.

Table 4 shows an overall mass balance delivered by the fluidized bed catalytic oxy-combustion simulation model of textile waste with carbon capture.

Unlike traditional combustion, oxy-combustion uses pure oxygen instead of air, which implies a significant economic cost due to the need to separate oxygen from air.²⁷ This process allows a more complete oxidation, notably reducing CO formation and generating mainly H₂O and CO₂ as products.²⁸ To maintain the system's efficiency without compromising its environmental performance, the amount of

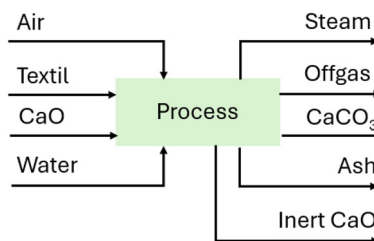
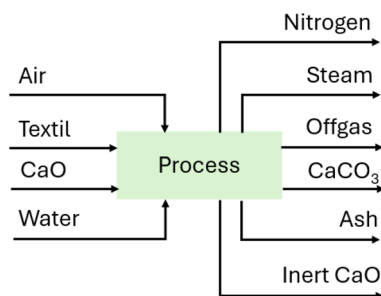


Fig. 7 Overall diagram of material inputs and outputs for textile waste's fluidized bed catalytic combustion process with carbon capture.



Table 3 Mass balance of fluidized bed catalytic combustion of textile waste with carbon capture

Component	Air	Textile	CaO	Water	Steam	Off-gas	CaCO ₃	Ash	Inert CaO
Mass flow (kg h ⁻¹)	1353	200	500	600	600	1393	357	3	300

**Fig. 8** Overall diagram of material inputs and outputs for textile waste's fluidized bed catalytic oxy-combustion process with carbon capture.

air fed to the separation unit was reduced, adapting to the specific conditions of the oxy-combustion process.²⁹ In addition, by eliminating nitrogen from the inlet flow, the volume of exhaust gases decreases compared to traditional combustion, which reduces the energy carried by these gases. Consequently, it was necessary to adjust the water feed to obtain steam with a quality similar to that generated in traditional combustion.

Table 5 shows a mass balance of the catalytic combustion process of textile waste in a fluidized bed with carbon capture. The COTTON and POLY streams are the textile waste feed, corresponding to 100 kg h⁻¹ of cotton and 100 kg h⁻¹ of polyester; the airflow, AIR stream, corresponds to 1353 kg h⁻¹, considering a 10% excess of air concerning the stoichiometric quantity.

The combustion gases corresponding to the S4 stream have 25% CO₂ in their composition, the main greenhouse gas generated during the combustion of organic materials, such as textile waste. A value of 392 kg h⁻¹ of CO₂ indicates a significant emission, reflecting that the burned textile waste contains a considerable amount of carbon, exceeding those reported in ref. 11 for textile waste, due to the higher carbon content in synthetic fibers. The chemical composition of textiles, especially synthetics, may contribute to these high CO₂ levels.¹ The O₂ concentration of 2.6% is low compared to other flue gases. However, this value indicates sufficient O₂ in the combustion air for complete combustion.¹⁷ The water in the flue gas indicates proper combustion since water is formed in a combustion reaction, and the low amount, 4.7%,

indicates low humidity of the combusted textile waste.¹ The low presence of SO₂ and ash, 0.3% and 0.2%, respectively, is positive, indicating that the textile waste does not contain large amounts of sulfur or minerals that could generate additional contamination.^{1,11} NO_x levels are minimal, <0.1%, suggesting that combustion conditions, such as temperature and oxygen supply, are controlled, which minimizes the emission of these compounds into the air, which are pollutants.¹⁰

In the S10 stream leaving the SCR, the NO_x content was reduced to N₂, thanks to the action of zeolite, which acts as a catalyst,¹³ decreasing these environmentally harmful components and precursors of acid rain.

In carbon capture with quicklime, CaO, the OFFGAS stream gases have approximately 40% less CO₂ than the S4 stream gases mentioned above because approximately 55% of the quicklime is useful lime.²⁵

Due to the energy exchange between the textile waste flue gas, the S4 stream, and the water in the WATER stream, it is possible to produce 600 kg h⁻¹ of superheated steam.

Table 6 shows a mass balance of the process of catalytic oxy-combustion of textile waste in a fluidized bed with carbon capture. The COTTON and POLY streams are the textile waste feed, and it can be observed that it corresponds to 100 kg h⁻¹ of cotton and 100 kg h⁻¹ of polyester; the airflow, AIR stream corresponds to 1255 kg h⁻¹ and an excess of 2% of air is added for the stoichiometric quantity, to reduce costs of oxygen separation. Only 295 kg h⁻¹ of O₂ enters the REACTOR unit, thanks to a separator unit called SEP that separates the N₂ from the air.

In the oxy-combustion gases corresponding to stream S4, CO₂ is the predominant gas, with a proportion of 79%, characteristic of oxy-combustion and suggesting efficient conversion of carbon in waste.³⁰ With the use of O₂-enriched air for oxy-combustion, the main composition of the flue gas is CO₂, water, dust, and SO₂; electrostatic precipitators and desulfurization methods can remove the dust and SO₂, and the remaining gases containing a high concentration of CO₂ can be more easily compressed, transported, and stored.³¹ Residual O₂ reaches 4%, indicating a slight excess of oxygen to ensure complete combustion. H₂O represents 14.0%, generated by both moisture in the residues and combustion of organic compounds. Small amounts of N₂ and SO₂ reflect the composition of the textile waste, while CO, NO, and NO₂

Table 4 Mass balance of fluidized bed catalytic oxy-combustion of textile waste with carbon capture

Component	Air	Textile	CaO	Water	Nitrogen	Steam	Off-gas	CaCO ₃	Ash	Inert CaO
Mass flow (kg h ⁻¹)	1255	200	500	280	960	280	335	357	3	300



Table 5 Mass balance (kg h^{-1}) for catalytic combustion of textile waste in a fluidized bed with carbon capture

	POLY	COTTON	AIR	STEAM	S1	S2	S3	S4	S5	S6	S7	S8	S9	S10	S11	S12	S13	S14	WATER	ZEOLITE	ASH	CAO	CACO ₃	OFFGAS	
Cotton	0	100	0	0	0	0	0	0	0	0	0	0	0	0	0	0	0	0	0	0	0	0	0	0	
Polyester	100	0	0	0	0	0	0	0	0	0	0	0	0	0	0	0	0	0	0	0	0	0	0	0	
CO ₂	0	0	0	0	0	0	0	391.9	391.9	0	391.9	0	391.9	391.9	391.9	0	0	0	0	0	0	0	0	235.2	
CO	0	0	0	0	0	0	0	0	0	0	0	0	0	0	0	0	0	0	0	0	0	0	0	0	
O ₂	0	0	318.2	0	31.6	43.7	75.3	44.1	44.1	0	44.1	0	44.1	44.2	44.2	0	318.2	0	0	0	0	0	0	0	44.2
H ₂ O	0	0	600	2.1	0.6	2.7	72.5	72.5	72.5	600	72.5	600	72.5	72.5	72.5	600	0	600	0	0	0	0	0	0	72.5
N ₂	0	0	1034.7	0	0.7	0.8	1.5	1036.1	1036.1	0	1036.1	0	1036.1	1036.2	1036.2	0	1034.7	0	0	0	0	0	0	0	1036.1
C	0	0	0	0	58.1	48.8	106.9	0	0	0	0	0	0	0	0	0	0	0	0	0	0	0	0	0	0
NO ₂	0	0	0	0	0	0	0	0	0	0	0	0	0	0	0	0	0	0	0	0	0	0	0	0	0
NO	0	0	0	0	0	0	0	0	0	0	0	0	0	0	0	0	0	0	0	0	0	0	0	0	0
SO ₂	0	0	0	0	0	0	0	4.8	4.8	0	4.8	0	4.8	4.8	4.8	0	0	0	0	0	0	0	0	0	4.8
H ₂	0	0	0	0	3.8	4	8	0	0	0	0	0	0	0	0	0	0	0	0	0	0	0	0	0	0
S	0	0	0	0	1.5	0.9	2.4	0	0	0	0	0	0	0	0	0	0	0	0	0	0	0	0	0	0
Ash	0	0	0	0	2.1	1.1	3.2	3.2	3.2	0	3.2	0	3.2	3.2	3.2	0	0	0	0	0	0	3.2	0	0	0
Zeolite	0	0	0	0	0	0	0	0	0	0	0	0	0	0	0	0	0	0	0	78	0	0	0	0	0
CaO	0	0	0	0	0	0	0	0	0	0	0	0	0	0	0	0	0	0	0	0	0	0	0	0	0
CaCO ₃	0	0	0	0	0	0	0	0	0	0	0	0	0	0	0	0	0	0	0	0	0	500	0	0	0
Mass flow	100	100	1353	600	100	100	200	1553	1553	600	1553	600	1553	1553	1550	600	1353	600	78	78	3.2	500	357	1393	
Temp (°C)	25	25	25	228	1000	1000	1000	1000	600	188	400	188	150	150	150	85	25	85	25	25	150	25	148	148	

Table 6 Mass balance (kg h^{-1}) for catalytic oxy-combustion of textile waste in a fluidized bed with carbon capture

	POLY	COTTON	AIR	STEAM	N ₂	S1	S2	S3	S4	S5	S6	S7	S8	S9	S10	S11	S12	S13	S14	WATER	ZEOLITE	ASH	CAO	CACO ₃	OFFGAS	
Cotton	0	100	0	0	0	0	0	0	0	0	0	0	0	0	0	0	0	0	0	0	0	0	0	0	0	
Polyester	100	0	0	0	0	0	0	0	0	0	0	0	0	0	0	0	0	0	0	0	0	0	0	0	0	
CO ₂	0	0	0	0	0	0	0	0	391.9	391.9	0	391.9	0	391.9	391.9	391.9	0	0	0	0	0	0	0	0	235.1	
CO	0	0	0	0	0	0	0	0	0	0	0	0	0	0	0	0	0	0	0	0	0	0	0	0	0	
O ₂	0	0	295.2	0	31.6	43.7	75.3	21.1	21.1	0	21.1	0	21.1	21.1	21.1	21.1	0	295.2	295.2	0	0	0	0	0	0	21.1
H ₂ O	0	0	280	2.1	0.6	2.7	72.5	72.5	72.5	280	72.5	280	72.5	280	72.5	280	0	280	0	280	0	0	0	0	0	72.5
N ₂	0	0	959.8	0	959.8	0.7	0.8	1.5	1.5	0	1.5	0	1.5	1.5	1.5	1.5	0	959.8	0	0	0	0	0	0	1.5	
C	0	0	0	0	58.1	48.8	106.9	0	0	0	0	0	0	0	0	0	0	0	0	0	0	0	0	0	0	
NO ₂	0	0	0	0	0	0	0	0	0	0	0	0	0	0	0	0	0	0	0	0	0	0	0	0	0	
NO	0	0	0	0	0	0	0	0	0	0	0	0	0	0	0	0	0	0	0	0	0	0	0	0	0	
SO ₂	0	0	0	0	0	0	0	0	4.8	4.8	0	4.8	0	4.8	4.8	4.8	0	0	0	0	0	0	0	0	4.8	
H ₂	0	0	0	0	3.8	4	8	0	0	0	0	0	0	0	0	0	0	0	0	0	0	0	0	0	0	
S	0	0	0	0	1.5	0.9	2.4	0	0	0	0	0	0	0	0	0	0	0	0	0	0	0	0	0	0	
Ash	0	0	0	0	2.1	1.1	3.2	3.2	3.2	0	3.2	0	3.2	3.2	3.2	3.2	0	0	0	0	0	3.2	0	0	0	
Zeolite	0	0	0	0	0	0	0	0	0	0	0	0	0	0	0	0	0	0	0	25	0	0	0	0	0	
CaO	0	0	0	0	0	0	0	0	0	0	0	0	0	0	0	0	0	0	0	0	0	0	0	0	0	
CaCO ₃	0	0	0	0	0	0	0	0	0	0	0	0	0	0	0	0	0	0	0	0	0	500	0	0	0	
Mass flow	100	100	1255	280	960	100	100	200	495	495	280	495	280	495	495	492	280	1255	295	280	25	3.2	500	357	335	
Temp (°C)	25	25	25	230	25	1200	1200	1200	600	188	400	188	150	150	150	85	25	85	25	85	25	150	25	148	148	



emissions are negligible (<0.1%), suggesting low emissions of pollutants typical of oxy-combustion.³⁰

In the S10 stream leaving the SCR, the NO_x content (<0.1%) was reduced to N₂, thanks to the action of zeolite, which acts as a catalyst,¹³ decreasing these environmentally harmful components and precursors of acid rain. In carbon capture with quicklime, CaO, the OFFGAS stream gases have approximately 40% less CO₂ than the S4 stream gases mentioned above because approximately 55% of the quicklime is useful lime.²⁵ The energy exchange between the textile waste flue gas (S4 stream) and water allows for producing 280 kg h⁻¹ of superheated steam.

The model does not consider catalyst deactivation; however, catalysts decrease in performance over time. The deactivation kinetics depend on the deactivation mechanism, catalyst type, and specific application. The primary zeolite deactivation mechanism reported in the literature is coke fouling, caused by accumulation within the micropores, which block active sites and impede molecular transport, leading to reduced activity and selectivity.^{32,33} In similar processes, a loss of up to 50–60% of catalytic activity has been reported after 200 hours of operation.³⁴ In the case of catalytic combustion of textile waste, there is latent poisoning by chlorinated compounds (dioxins and furans) which, unlike coke fouling, may be irreversible.³⁵

In the process industry, it is common to implement periodic cycles of regeneration by controlled coke oxidation, which allows partial recovery of zeolite activity. The frequency and effectiveness of these regenerations depend on the operating conditions and the type of coke formed.³³ In cases where regeneration is insufficient, total or partial replacement of the catalyst may be necessary. According to the literature, a conservative estimate of total catalyst replacement is 2–4 years for selective catalytic reduction.³⁶

Also, the model does not consider the gradual deactivation of CaO in the carbon capture stage, the literature reports that CaO suffers deactivation and loss of capacity after some regeneration cycles, due to the blockage of the internal pores, mainly by sintering, which increases the resistance to CO₂ diffusion through the CaCO₃ layers.^{37,38} Experimentally, it has been shown that the CO₂ capture capacity can be reduced by up to 85–90% after 10 regeneration cycles, depending on the process conditions.³⁹

At the industrial level, rigorous monitoring of the adsorption capacity of CaO and a plan for partial replacement and periodic regeneration of the beds is required so as not to compromise the carbon capture capacity. CaO is considered depleted with at most 30% efficiency loss. Since the typical initial adsorption capacity of 0.3–0.7 g CO₂ per g CaO,³⁹ a replacement plan would become necessary depending on the number of cycles. Although this phenomenon does not affect the instantaneous balances of the process, it affects the overall efficiency and long-term economic viability.

Although the study focused on CO₂ and NO_x emissions from the combustion of textile waste, it is essential to

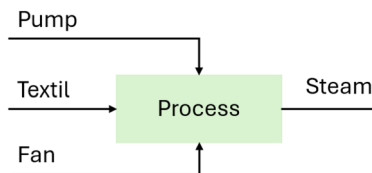


Fig. 9 Overall diagram of energy inputs and outputs for textile waste's fluidized bed catalytic combustion process with carbon capture.

recognize that this process can also generate other pollutants, such as dioxins, furans, and heavy metals. While such compounds were not modeled in Aspen Plus, evidence supporting their possible formation and available technologies for their mitigation has been incorporated into the literature review.

The literature reports that the combustion of textile wastes such as cotton and polyester can generate dioxins and furans in the order of 259.74 pg g⁻¹ for cotton and 1400.3 pg g⁻¹ for polyester under non-optimized conditions.⁴⁰ Several studies indicate that catalysts such as VO_x/WO_x/TiO₂ or certain types of zeolites can reduce NO_x, dioxins, and furans emissions by at least 90%.¹³ Heavy metals are usually concentrated in the ashes and can be separated by technologies such as baghouses, cyclones, or electrostatic precipitators, which have efficiencies greater than 99%.^{10,41} For a possible implementation on an industrial scale, an integral emission control system that combines these technologies will be required, ensuring compliance with environmental regulations and the technical feasibility of the process.

Fig. 9 shows an overall diagram of the combustion process for energy inputs and outputs to calculate overall process efficiency.

Table 7 shows an overall energy balance for catalytic fluidized bed combustion of textile waste with carbon capture.

From the information provided in Table 7 and eqn (1), an overall process efficiency of 40% is obtained. This efficiency could decrease considering the size reduction stage of the textile waste.

Fig. 10 shows an overall diagram of the oxy-combustion process for energy inputs and outputs to calculate overall process efficiency.

Table 8 shows an overall energy balance for catalytic oxy-combustion of textile waste in a fluidized bed with carbon capture.

The information provided in Table 8 and eqn (1) shows an overall process efficiency of 18%. This efficiency could

Table 7 Energy balance for catalytic fluidized bed combustion of textile waste with carbon capture

Component	Input			Output
	Textile	Pump	Fan	Steam
Energy	20.5 MJ kg ⁻¹	0.5 kW	83 kW	2.9 MJ kg ⁻¹
Mass flow	200 kg h ⁻¹	600 kg h ⁻¹	1353 kg h ⁻¹	600 kg h ⁻¹
Energy flow	4100 MJ h ⁻¹	1.8 MJ h ⁻¹	299 MJ h ⁻¹	1740 MJ h ⁻¹



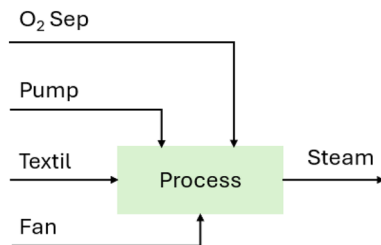


Fig. 10 Overall diagram of energy inputs and outputs for the catalytic oxy-combustion process of textile waste in a fluidized bed with carbon capture.

decrease considering the size reduction stage of the textile waste.

A key aspect of the proposed process is the generation of superheated steam as a form of energy. In the case of catalytic combustion, a production of 600 kg h^{-1} of steam is estimated, which opens opportunities for its integration into industrial thermal networks. This steam can be used for internal process applications (such as waste drying, air preheating, heat exchangers) or sold to other chemical industries. Additionally, implementing cogeneration systems would allow the steam to be transformed into electrical energy, contributing to the technical and economic viability of the process.

For the technical assessment of the catalytic combustion process of textile waste with carbon capture, the combustion of textile waste in a fixed-bed reactor is used as a reference.

Fig. 11 compares the flue gases from the proposed configurations and the fixed bed reactor (case 1).

Concerning CO_2 , case 2 has 17.8% compared to case 1, which has 18%, but it must be considered that the case 1 gases contain 3% CO, which indicates that the case 1 combustion is incomplete, and if it were complete, CO_2 would increase to the order of 20% in the case 1. On the other hand, case 3 has 90% CO_2 , which is in agreement with the literature since, in this way, it is easier to separate the CO_2 from the combustion gases and store it later.¹⁴

Concerning CO, the values were normalized to eliminate scaling problems.⁴² Both cases 2 and 3 have an order of 1%, compared to case 1, which has 3% CO, indicating incomplete combustion. Case 2, in terms of specific amounts of CO, has on the order of 0.4 mg CO per kg textile, which agrees with.²⁹ The CO of case 1 is influenced because a fixed bed reactor is used, in which the textile waste is not agitated, compared to the proposed fluidized bed reactor. It is worth mentioning that the proposed fixed-bed reactor reaches temperatures on

the order of $800 \text{ }^\circ\text{C}$ compared to the proposed fluidized-bed reactor operating at $1000 \text{ }^\circ\text{C}$, which promotes the oxidation of the material.

Concerning O_2 , case 2 has 3%, which is very similar to the flue gas in case 1, which has 4%; however, in case 1, complete combustion is not achieved since combustion is performed in a fixed bed reactor. Case 3 has 8% O_2 , which is expected since oxygen-enriched air is supplied to the reactor; however, this value can be optimized, since it involves an economic cost to separate O_2 .

This study evaluates a textile waste blend of 50% cotton and 50% polyester as a base case, supported by information reported in the literature. An analysis of the effect of the gradual increase of polyester in the composition of the textile blend from 0% to 100% is shown in Fig. 12. In this analysis, the generated steam flow is considered fixed, and the fed air is adjusted according to the composition of the textile blend to ensure complete combustion.

It is visualized that CO_2 increases as the polyester content in the textile blend increases, from 214.7 kg h^{-1} (0% polyester) to 255.6 kg h^{-1} (100% polyester), which could be because polyester has a higher carbon content in its elemental composition.

Up to 40% polyester, the process becomes less efficient. This happens because not enough energy is generated to improve the efficiency of the process. However, when the percentage of polyester increases from 40% to 100%, the efficiency gradually improves as more energy is produced in the system. However, there are no significant variations in efficiency in the process; the average efficiency is in the order of 40%.

In this study, only a temperature of $1000 \text{ }^\circ\text{C}$ and 2 bar of pressure inside the combustion reactor is evaluated, with the support of information reported in the literature. Fig. 13 shows an analysis where the temperature is gradually increased, keeping the pressure constant at 2 bar. Fig. 14 shows an analysis where the pressure is gradually increased, keeping the temperature constant at $1000 \text{ }^\circ\text{C}$. These analyses keep the composition of the feed mixture constant at 50% cotton/50% polyester, the air flow rate fed, and the steam flow rate generated.

In Fig. 13, it is shown that the CO_2 generated in the offgases remains constant at 17% as the temperature increases, because the combustion reaction goes in one direction only, and stops when the fuel is exhausted. The efficiency of the process increases, since the steam generated has more enthalpy, according to eqn (1).

Table 8 Energy balance for catalytic oxy-combustion of textile wastes in a fluidized bed with carbon capture

Component	Input				Output
	Textile	Pump	Fan	O_2 Sep	Steam
Energy	20.5 MJ kg^{-1}	0.2 kW	77 kW	$0.2 \text{ kWh kg}^{-1} \text{ O}_2$	2.9 MJ kg^{-1}
Mass flow	200 kg h^{-1}	280 kg h^{-1}	1255 kg h^{-1}	295 kg h^{-1}	280 kg h^{-1}
Energy flow	4100 MJ h^{-1}	0.7 MJ h^{-1}	277 MJ h^{-1}	212 MJ h^{-1}	812 MJ h^{-1}



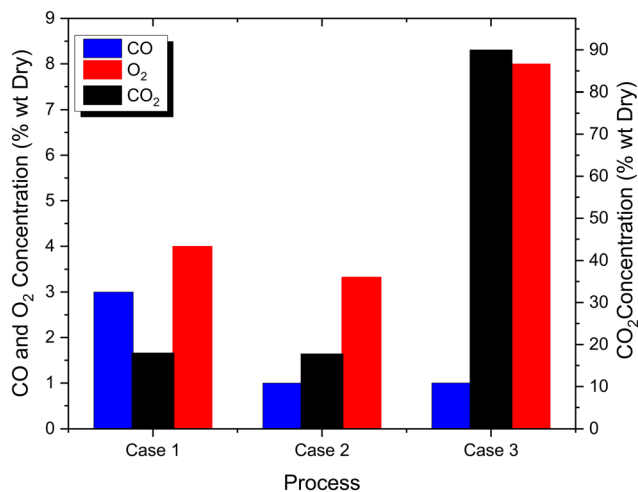


Fig. 11 Technical comparison of CO₂, CO, and O₂ gases for reference processes (case 1) combustion (case 2) and oxy-combustion (case 3).

In Fig. 14, it is shown that the CO₂ generated in the offgases remains constant at 17% as the pressure increases, because the combustion reaction goes in one direction only, and stops when the fuel is exhausted. Concerning the process efficiency, since the temperature inside the reactor is kept constant at 1000 °C, it does not produce an increase in the enthalpy of the steam generated, therefore, the process efficiency remains constant.

At the industrial level, the implementation of the process faces several technical and logistical barriers, including variability in waste composition, the need for efficient size reduction to ensure homogeneous combustion, and operational challenges in fluidized bed reactors, such as sintering and fouling. In addition, proper integration with existing infrastructure is required, especially in steam distribution systems, and economic and energy constraints associated with oxygen production for oxy-combustion are faced. These difficulties must be carefully considered in the design and planning of the process.

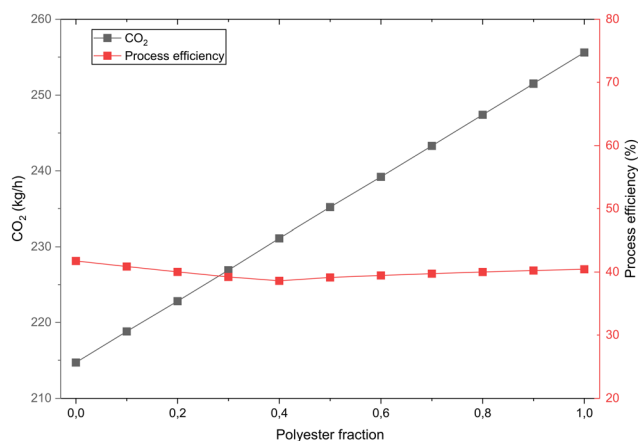


Fig. 12 Polyester fraction vs. CO₂ flux in off-gas and process efficiency.

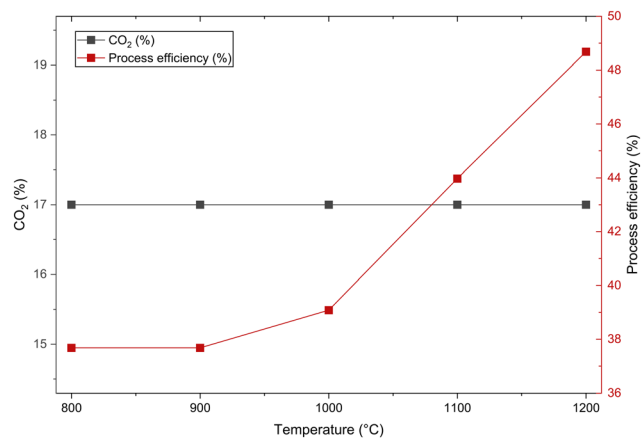


Fig. 13 Reactor temperature vs. % CO₂ and process efficiency (at 2 bar).

Compared to other revalorization technologies such as pyrolysis or gasification, the proposed process has advantages from an environmental and economic point of view.

Pyrolysis and gasification face significant operational limitations due to the heterogeneous composition of textile waste, which affects the quality and stability of the obtained products (bio-oil or synthesis gas), as well as the need for rigorous process control.^{1,18–20} In addition, both technologies require high temperatures (around 500 °C for pyrolysis and up to 1200 °C for gasification), high energy consumption, and the use of inert or reactive gases such as N₂, CO₂, or steam, which significantly increases operational costs.^{1,43,44} In particular, synthetic textile wastes, such as PET and nylon, are less reactive in pyrolysis and generate hazardous compounds, representing an additional environmental disadvantage.⁴⁵

In contrast, fluidized bed catalytic combustion benefits from higher thermal stability and better air/fuel mixing. Using catalysts improves selectivity towards desired gaseous products, such as CO₂ and H₂O. In addition, by integrating carbon capture, the carbon footprint of the process is

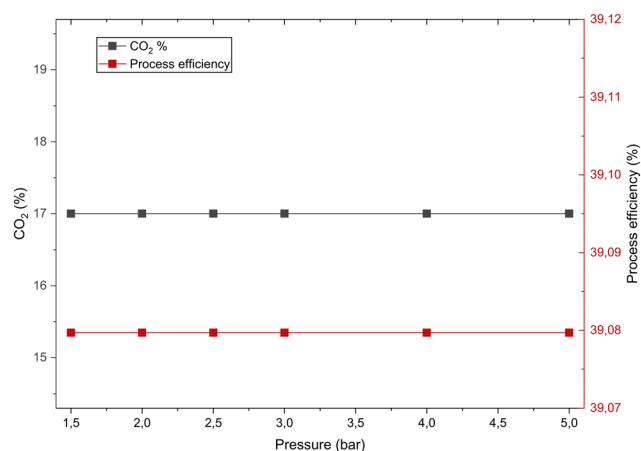


Fig. 14 Reactor pressure vs. % CO₂ and process efficiency (at 1000 °C).



significantly mitigated. From an economic point of view, the reduced complexity in product conditioning and the potential for valorization of the heat generated offset the costs associated with the CO₂ capture system.

4. Conclusions

This study assessed the viability of energetically valorizing textile waste using fluidized bed catalytic combustion with carbon capture. This provides a technically feasible alternative. It also promotes environmentally responsible waste management.

The results show that fluidized bed catalytic combustion effectively manages mixed textile waste, achieves complete combustion, low emissions of pollutants (CO, NO_x, SO₂), and efficient energy recovery in superheated steam (600 kg h⁻¹). The overall energy efficiency of the catalytic combustion process reached 40%, primarily due to the optimized use of the textile waste's calorific value and efficient heat exchange, indicating a strong potential for energy integration in industrial settings.

In contrast, while beneficial in producing a CO₂-rich flue gas that simplifies capture and storage, catalytic oxy-combustion showed a lower overall efficiency of 18%, mainly due to the high energy demand of oxygen separation from air. This highlights the trade-off between ease of CO₂ capture and energy consumption.

Carbon capture using CaO proved effective, reducing CO₂ emissions by approximately 40%, which supports climate change mitigation efforts. Moreover, zeolite-based SCR successfully reduced NO_x emissions to environmentally benign N₂, demonstrating the catalytic system's capacity to minimize harmful secondary pollutants.

Compared to traditional fixed-bed combustion, the proposed fluidized bed setup significantly improved combustion uniformity and pollutant control, validating its technical superiority for textile waste valorization.

Although the simulations indicate promising performance, further studies are necessary to address operational challenges such as CaO deactivation and to optimize reactor conditions. These findings establish a solid foundation for continued research aimed at scaling up and improving the process, contributing to developing sustainable waste management solutions, and promoting a circular economy.

Conflicts of interest

There are no conflicts of interest to declare.

Data availability

The data supporting the findings of this study, including the experimental results and process simulations, are available in the manuscript. The simulation software was Aspen Plus® V14. Additional supporting data, including process flow diagrams and mass balances, have been included as part of the article.

Acknowledgements

The National Commission for Scientific and Technological Research in Chile funded this study through FONDECYT REGULAR 1230656 and ANID BECAS/DOCTORADO NACIONAL 21242170.

References

- 1 P. Athanapoulos and A. Zabanitou, Post-consumer textile thermochemical recycling to fuels and biocarbon: A critical review, *Sci. Total Environ.*, 2022, **834**, 155387, DOI: [10.1016/j.scitotenv.2022.155387](https://doi.org/10.1016/j.scitotenv.2022.155387).
- 2 European Parliament, The impact of textile production and waste on the environment (infographics). Accessed: Apr. 24, 2024, [Online]. Available: <https://www.europarl.europa.eu/topics/en/article/20201208STO93327/the-impact-of-textile-production-and-waste-on-the-environment-infographics>.
- 3 Ellen MacArthur Foundation, A new textiles economy: Redesigning fashion's future. [Online]. Available: <https://www.ellenmacarthurfoundation.org/a-new-textiles-economy>.
- 4 B. Ütebay, P. Çelik and A. Çay, Effects of cotton textile waste properties on recycled fibre quality, *J. Cleaner Prod.*, 2019, **222**, 29–35, DOI: [10.1016/j.jclepro.2019.03.033](https://doi.org/10.1016/j.jclepro.2019.03.033).
- 5 Ministerio del Medio Ambiente, '¡Adiós al Fast Fashion!... ¡Bienvenida Moda Sostenible!' Accessed: Apr. 24, 2024, [Online]. Available: <https://mma.gob.cl/adios-al-fast-fashion-bienvenida-moda-sostenible/>.
- 6 B. Piribauer and A. Bartl, Textile recycling processes, state of the art and current developments: A mini review, *Waste Manage. Res.*, 2019, **37**(2), 112–119, DOI: [10.1177/0734242X18819277](https://doi.org/10.1177/0734242X18819277).
- 7 D. I. Alves, M. Barreiros, R. Fanguero and D. P. Ferreira, Valorization of textile waste: non-woven structures and composites, *Front. Environ. Sci.*, 2024, **12**, 2024, DOI: [10.3389/fenvs.2024.1365162](https://doi.org/10.3389/fenvs.2024.1365162).
- 8 K. Makavou, The EU is clear: Waste-To-Energy incineration has no place in the sustainability agenda. [Online]. Available: <https://zerowasteurope.eu/2021/05/wte-incineration-no-place-sustainability-agenda/>.
- 9 S. Yasin and D. Sun, Propelling textile waste to ascend the ladder of sustainability: EOL study on probing environmental parity in technical textiles, *J. Cleaner Prod.*, 2019, **233**, 1451–1464, DOI: [10.1016/j.jclepro.2019.06.009](https://doi.org/10.1016/j.jclepro.2019.06.009).
- 10 L. Makarichi, W. Jutidamrongphan and K. a. Techato, The evolution of waste-to-energy incineration: A review, *Renewable Sustainable Energy Rev.*, 2018, **91**, 812–821, DOI: [10.1016/j.rser.2018.04.088](https://doi.org/10.1016/j.rser.2018.04.088).
- 11 C. Ryu, A. N. Phan, V. N. Sharifi and J. Swithenbank, Combustion of textile residues in a packed bed, *Exp. Therm. Fluid Sci.*, 2007, **31**(8), 887–895, DOI: [10.1016/j.expthermflusci.2006.09.004](https://doi.org/10.1016/j.expthermflusci.2006.09.004).
- 12 H. Goodfellow and E. Tähti, *Industrial Ventilation Design Guidebook*, Academic Press, 2001, pp. 677–806, DOI: [10.1016/B978-012289676-7/50012-6](https://doi.org/10.1016/B978-012289676-7/50012-6).
- 13 M. Gallastegi, VO_x/WO_x/TiO₂ and alternative catalysts for the simultaneous abatement of NO_x and PCDD/Fs from



- MWS treatment plants, *Ph.D Thesis*, Universidad del País Vasco, 2016.
- 14 D. Bose, R. Bhattacharya, T. Kaur, R. Pandya, A. Sarkar, A. Ray and S. Mondal, Innovative approaches for carbon capture and storage as crucial measures for emission reduction within industrial sectors, *Carbon Capture Sci. Technol.*, 2024, **12**, 100238, DOI: [10.1016/j.ccst.2024.100238](https://doi.org/10.1016/j.ccst.2024.100238).
 - 15 L. Zaccariello and F. Montagnaro, Fluidised bed gasification of biomasses and wastes to produce hydrogen-rich syn-gas – a review, *J. Chem. Technol. Biotechnol.*, 2023, **98**, 1878–1887, DOI: [10.1002/jctb.7393](https://doi.org/10.1002/jctb.7393).
 - 16 B. Leckner and F. Lind, Combustion of municipal solid waste in fluidized bed or on grate – A comparison, *Waste Manage.*, 2020, **109**(2020), 94–108, DOI: [10.1016/j.wasman.2020.04.050](https://doi.org/10.1016/j.wasman.2020.04.050).
 - 17 C. Ryu, A. N. Phan, V. N. Sharifi and J. Swithenbank, Co-combustion of textile residues with cardboard and waste wood in a packed bed, *Exp. Therm. Fluid Sci.*, 2007, **32**(2), 450–458, DOI: [10.1016/j.expthermflusci.2007.05.008](https://doi.org/10.1016/j.expthermflusci.2007.05.008).
 - 18 J. Xu, N. Brodu, L. Abdelouahed and B. Taouk, Investigation of the combination of fractional condensation and water extraction for improving the storage stability of pyrolysis bio-oil, *Fuel*, 2022, **314**, 123019, DOI: [10.1016/j.fuel.2021.123019](https://doi.org/10.1016/j.fuel.2021.123019).
 - 19 R. Sakthivel, K. Ramesh, P. Mohamed Shameer and R. Purnachandran, Experimental investigation on improvement of storage stability of bio-oil derived from intermediate pyrolysis of Calophyllum inophyllum seed cake, *J. Energy Inst.*, 2019, **92**(3), 768–782, DOI: [10.1016/j.joei.2018.02.006](https://doi.org/10.1016/j.joei.2018.02.006).
 - 20 C. Vela, I. Maric and J. Seemann, *Valorisation of textile waste via steam gasification in a fluidized bed reactor*, 2019.
 - 21 Y. Sakurai, T. Ito and M. Nishimoto, Pyrolysis characteristics of blended textile in waste clothing, *J. Energy Inst.*, 2025, **120**, 102042, DOI: [10.1016/j.joei.2025.102042](https://doi.org/10.1016/j.joei.2025.102042).
 - 22 V. S. N. S. Goli, D. N. Singh and T. Baser, A critical review on thermal treatment technologies of combustible fractions from mechanical biological treatment plants, *J. Environ. Chem. Eng.*, 2021, **9**(4), 105643, DOI: [10.1016/j.jece.2021.105643](https://doi.org/10.1016/j.jece.2021.105643).
 - 23 N. Trueba, Dopaje de catalizadores basados en Mn y Ce para la depuración simultánea de NO_x PCDD/Fs en plantas de RSU, 2019.
 - 24 D. Kunni and O. Levenspiel, *Fluidization engineering*, Elsevier, 2013.
 - 25 P. Kong, *et al.*, Insight into the deactivation mechanism of CaO-based CO₂ sorbent under in-situ coal combustion, *Sep. Purif. Technol.*, 2024, **346**, 127529, DOI: [10.1016/j.seppur.2024.127529](https://doi.org/10.1016/j.seppur.2024.127529).
 - 26 Y. A. Cengel, *Termodinámica*, 2019.
 - 27 I. Pfaff and A. Kather, Comparative thermodynamic analysis and integration issues of CCS steam power plants based on oxy-combustion with cryogenic or membrane based air separation, *Energy Procedia*, 2009, **1**(1), 495–502, DOI: [10.1016/j.egypro.2009.01.066](https://doi.org/10.1016/j.egypro.2009.01.066).
 - 28 C. W. Ong and C. L. Chen, Intensification, optimization and economic evaluations of the CO₂-capturing oxy-combustion CO₂ power system integrated with the utilization of liquefied natural gas cold energy, *Energy*, 2021, **234**, 121255, DOI: [10.1016/j.energy.2021.121255](https://doi.org/10.1016/j.energy.2021.121255).
 - 29 S. W. Grass and B. M. Jenkins, Biomass fueled fluidized bed combustion: Atmospheric emissions, emission control devices and environmental regulations, *Biomass Bioenergy*, 1994, **6**(4), 243–260, DOI: [10.1016/0961-9534\(94\)90064-7](https://doi.org/10.1016/0961-9534(94)90064-7).
 - 30 A. Krishnan, A. Nighojkar and B. Kandasubramanian, Emerging towards zero carbon footprint via carbon dioxide capturing and sequestration, *Carbon Capture Sci. Technol.*, 2023, **9**, 100137, DOI: [10.1016/j.ccst.2023.100137](https://doi.org/10.1016/j.ccst.2023.100137).
 - 31 D. Y. C. Leung, G. Caramanna and M. M. Maroto-Valer, An overview of current status of carbon dioxide capture and storage technologies, *Renewable Sustainable Energy Rev.*, 2014, **39**, 426–443, DOI: [10.1016/j.rser.2014.07.093](https://doi.org/10.1016/j.rser.2014.07.093).
 - 32 S. Fan, H. Wang, S. Wang, M. Dong and W. Fan, Recent progress in the deactivation mechanism of zeolite catalysts in methanol to olefins, *Sci. China: Chem.*, 2024, **67**(12), 3934–3943, DOI: [10.1007/s11426-024-2078-4](https://doi.org/10.1007/s11426-024-2078-4).
 - 33 A. Hwang and A. Bhan, Deactivation of Zeolites and Zeotypes in Methanol-to-Hydrocarbons Catalysis: Mechanisms and Circumvention, *Acc. Chem. Res.*, 2019, 2647–2656, DOI: [10.1021/acs.accounts.9b00204](https://doi.org/10.1021/acs.accounts.9b00204).
 - 34 M. He, M.-F. Ali, Y.-Q. Song, X.-L. Zhou, J. A. Wang, X.-Y. Nie and Z. Wang, Study on the deactivation mechanism of HZSM-5 in the process of catalytic cracking of n-hexane, *Chem. Eng. J.*, 2023, **451**, 138793, DOI: [10.1016/j.cej.2022.138793](https://doi.org/10.1016/j.cej.2022.138793).
 - 35 M. Jin, P. Wang, Z. Li, K. Li and Y. Liu, Deactivation mechanism of Cu-based zeolites (AEI, SSZ-13, ZSM-5, BEA) for NH₃-SCR by hydrocarbons deposition species, *Fuel*, 2024, **365**, 131215, DOI: [10.1016/j.fuel.2024.131215](https://doi.org/10.1016/j.fuel.2024.131215).
 - 36 M. D. Argyle and C. H. Bartholomew, Heterogeneous catalyst deactivation and regeneration: A review, *Catalysts*, 2015, **5**(1), 145–269, DOI: [10.3390/catal5010145](https://doi.org/10.3390/catal5010145).
 - 37 M. Alonso, N. Rodríguez, B. González, G. Grasa, R. Murillo and J. C. Abanades, Carbon dioxide capture from combustion flue gases with a calcium oxide chemical loop. Experimental results and process development, *Int. J. Greenhouse Gas Control*, 2010, **4**(2), 167–173, DOI: [10.1016/j.ijggc.2009.10.004](https://doi.org/10.1016/j.ijggc.2009.10.004).
 - 38 M. Heidari, M. Tahmasebpour, S. Borhan and C. Pevida, CO₂ capture activity of a novel CaO adsorbent stabilized with (ZrO₂ + Al₂O₃ + CeO₂)-based additive under mild and realistic calcium looping conditions, *J. CO₂ Util.*, 2021, **53**, 101747, DOI: [10.1016/j.jcou.2021.101747](https://doi.org/10.1016/j.jcou.2021.101747).
 - 39 A. Al-mamoori, S. Lawson, A. A. Rownaghi and F. Rezaei, Improving Adsorptive Performance of CaO for High-Temperature CO₂ Capture through Fe and Ga Doping, *Energy Fuels*, 2019, **33**(2), 1404–1413, DOI: [10.1021/acs.energyfuels.8b03996](https://doi.org/10.1021/acs.energyfuels.8b03996).
 - 40 J. Moltó, Descomposició tèrmica de residus tèxtils: estudi cinètic i formació de contaminants, *PhD Thesis*, Univ. Alicant., 2019, pp. 252–266.
 - 41 P. Ubilla, *Ingeniería en Ventilación y Filtración de Aire*, Aqualogy, Santiago, Chile, 2014.
 - 42 M. Kamber and J. Han, *Data Mining: Concepts and Techniques: Concepts and Techniques*, 2006.



- 43 G. Lopez, M. Artetxe, M. Amutio, J. Alvarez, J. Bilbao and M. Olazar, Recent advances in the gasification of waste plastics. A critical overview, *Renewable Sustainable Energy Rev.*, 2018, **82**(Part 1), 576–596, DOI: [10.1016/j.rser.2017.09.032](https://doi.org/10.1016/j.rser.2017.09.032).
- 44 S. Li, I. Cañete Vela, M. Järvinen and M. Seemann, Polyethylene terephthalate (PET) recycling via steam gasification – The effect of operating conditions on gas and tar composition, *Waste Manage.*, 2021, **130**, 117–126, DOI: [10.1016/j.wasman.2021.05.023](https://doi.org/10.1016/j.wasman.2021.05.023).
- 45 D. Kwon, S. Yi, S. Jung and E. E. Kwon, Valorization of synthetic textile waste using CO₂ as a raw material in the catalytic pyrolysis process, *Environ. Pollut.*, 2021, **268**, 115916, DOI: [10.1016/j.envpol.2020.115916](https://doi.org/10.1016/j.envpol.2020.115916).

